Chinese Journal of Chemistry, **2004**, *22*, 1158—1163 **Article**

Electrochemical Characteristics of $Mg_{0.9}Ti_{0.1-x}Zr_xNi$ (x=0.02, 0.04, 0.06) Alloys

YUAN, Hua-Tang[a,b](袁华堂) FENG, Yan*[,a,b](冯艳) QIAO, Lin-Jun[a,b](乔林军)
LIU, Qiang[a,b](刘强) WANG, Yi-Jing[a,b](王一菁)

[a] *Institute of New Energy Materials Chemistry, Nankai University, Tianjin 300071, China*
[b] *Unite Institute of Nankai-Tianjin University, Tianjin 300071, China*

Mg-based hydrogen storage alloys $Mg_{0.9}Ti_{0.1-x}Zr_xNi$ (x=0.02, 0.04, 0.06) were successfully prepared by means of mechanical alloying (MA). The effects of Zr addition on the discharge capacity and the cycle performance of the Mg-based electrodes were also studied. It was found that the discharge capacities were improved with addition of a small amount of Zr and the cycle performances of the alloy were stabilized with the addition of Ti. The effects of surface modification or coating on the properties of $Mg_{0.9}Ti_{0.06}Zr_{0.04}Ni$ were also studied. The results indicated that coating with graphite improved both the discharge capacity and cycle life of the amorphous $Mg_{0.9}Ti_{0.06}Zr_{0.04}Ni$ electrode.

Keywords Mg-based hydrogen storage, electrochemical property, surface coating, XRD, SEM, EDAX

Introduction

Mg-based hydrogen storage alloys are attractive materials for energy conversion and hydrogen storage because of their lighter weight, higher hydrogen storage capacity and lower cost compared to other series of hydrogen storage materials.[1]

In recent years, it was found that some amorphous Mg-Ni alloys prepared by mechanical alloying (MA) could absorb and desorb electrochemically a large amount of hydrogen at room temperature. Zhang *et al.*[2] reported that the Mg-Ni type alloys substituted with Zr possessed a high cycling capacity retention and a larger initial discharge capacity than original alloy $Mg_{35}Ti_{10}Ni_{55}$. Goo *et al.*[3] reported that the discharge capacity of $(Mg_{0.7}Zr_{0.3})_2$ reaches 530 mA•h•g^{-1}.

However, the practical application of Mg-based alloys is prevented by their poor hydriding/dehydriding kinetics at room temperature and their rapid degradation in alkaline solution. Those amorphous MA alloys make a new promise of research application of Mg-based alloys. The mechanism of degradation for amorphous Mg-Ni alloys and the methods to improve it have been widely studied at present.[4-7] Iwakura *et al.*[8] and Liu *et al.*[9] reported that the main reason for degradation of amorphous MgNi alloy is serious oxidation of magnesium and nickel by the electrolyte.

Surface coating is a kind of surface modification, which plays an important role in improving the surface activation of Mg-based hydrogen storage alloys, protecting alloys form oxidation and depressing the capacity degradation. Iwakura *et al.*[10] have studied electrochemical characterization of MgNi alloy which was surface modified with graphite, and it was reported that the discharge capacity of those alloys were improved. Han *et al.*[11] reported that the surface of the amorphous MgNi alloy was coated with Ti, Al and Zr by ball milling in order to improve the cycle life. Iwakura *et al.*[12] reported that $Mg_{0.9}Ti_{0.06}V_{0.04}Ni$-graphit composite exhibited better high-rate discharge ability and cycle performance than either $Mg_{0.9}Ti_{0.06}V_{0.04}Ni$ alloy or MgNi-graphite composite. These results indicate that both bulk and surface modifications of in the MgNi alloy are very effective in improving their hydrogen desorbability and charging-discharging characteristics.

In this paper, on the basis of the previous work, partial substitution of elements Ti and Zr for Mg and the surface modification with graphite were carried out in order to improve the electrode characteristics of MgNi amorphous alloys and the effects of Ti, Zr addition were investigated.

Experimental

MgNi and $Mg_{0.9}Ti_{0.1-x}Zr_xNi$ (x=0.02, 0.04, 0.06) alloys were prepared from mixed powder of pure Mg, Ni, Ti, and Zr by MA. Metal powders the purity of which was higher than 99% with sizes of 200 mesh were used. The experiment conditions were adopted as follows: the mixed pure metal powder with a ball to powder weight ratio of 20∶1 in a stainless steel vessel under an Ar atmosphere was milled for 80 h. The rolling

* E-mail: fengyan2002@eyou.com; Tel.: +86-022-23504527; Fax: +86-022-23502604
Received August 22, 2003; revised and accepted July 1, 2004.
Project supported by the National High '863' Project (No. 2001AA515022), the Major State Basic Research Development Program (No. G200026405) and the Union Fund of the Unite Institute of Nankai-Tianjin University.

speed of ball milling machine was 450 r/min. The containers (250 mL in volume) and balls (10—20 mm in diameter) were made of stainless steel.

The method of surface modification is that the MA 80 h alloys and 10 wt% graphite were mixed together in the stainless steel vessel with a ball to powder weight ratio of 100∶1 at a speed of 450 r/min under an Ar atmosphere for 1 h. The prepared powder was amorphized composite alloy, which was made of $Mg_{0.9}Ti_{0.06}Zr_{0.04}Ni$ alloy and graphite.

The crystal structure and surface configuration of the alloy were characterized by X-ray diffraction (Rigaku D/Max-2500, Cu Kα radiation), scanning electron microscopy (Hitachi X-650), and EDAX Falcon-60 energy apparatus.

The test electrodes were prepared by mixing the MA alloy powder with Ni powder in a mass ratio of 1∶3, and 0.6 g of the mixture was pressed under a pressure of 30 MPa into pellets of 10 mm in diameter. After that, both sides of the resulting pellet were covered with a foam nickel sheet (2×2 cm^2) and pressed at 20 MPa and soldered to a Ni wire to prepare a negative electrode. Charging-discharging cycle tests of the alloy electrodes were carried out in 5 mol/L KOH solution at room temperature. Electrochemical measurements were performed using an automatic land battery-testing instrument controlled by a computer. The electrochemical charge-discharge test has used a three-electrode system, a testing electrode, a $NiOOH/Ni(OH)_2$ counter electrode and Hg/HgO reference electrode. The preparation of the testing electrode and the measuring methods has been reported before.[13] Each negative electrode was charged at 100 $mA\cdot g^{-1}$ for 6 h and discharged to −0.5 V vs. Hg/HgO at 25 $mA\cdot g^{-1}$. The resting time between charging and discharging was 10 min.

Result and discussion

Structural characteristics

Figure 1 shows the XRD patterns of the MA 40 h MgNi and $Mg_{0.9}Ti_{0.1-x}Zr_xNi$ (x=0.02, 0.04, 0.06) alloys, and the XRD patterns of the MA 80 h alloys have been given in Figure 2. With the ball-milling time increasing, the peaks of MgNi and Ni become broader and less intense. All alloys exhibit a broad diffuse peak at around 40—45 degree, which implies that the partial substitution of MgNi by the elements of Ti and Zr studied does not change the amorphous major phase structure. All the alloys of MA 80 h exhibit a trace of elemental Ni except $Mg_{0.9}Ti_{0.04}Zr_{0.06}Ni$ alloy, that is to say, $Mg_{0.9}Ti_{0.04}Zr_{0.06}Ni$ alloy has been completely amorphized. This indicates that the partial substitution by Zr in MgNi type alloys can promote the extent of amorphism in those alloys.[14] That is because the atomic radius of Zr is larger than that of Mg or Ni. Therefore, Zr addition to MgNi type alloys may lead to severe volume expansion of MgNi lattice. Chakk *et al.*[15] advanced a model for amorphization by MA. During the mechanical alloying of $Mg_{0.9}Ti_{0.1-x}Zr_xNi$ (x=0.02, 0.04, 0.06) alloy, the Zr atom penetrates into the host MgNi lattice, which may occupy either a substitutional or interstitial site in the MgNi lattice. During ball milling of $Mg_{0.9}Ti_{0.1-x}Zr_xNi$ (x=0.02, 0.04, 0.06) alloys, the lattice strain is caused by comminution. The mechanical strain at room temperature can effectively destroy ordering of the host lattice with the help of the impurity Zr and Ti.

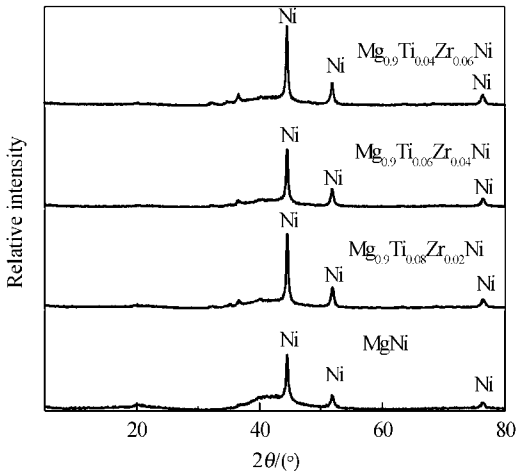

Figure 1 XRD pattern of MgNi, $Mg_{0.9}Ti_{0.1-x}Zr_xNi$ (x=0.02, 0.04, 0.06) by MA 40 h.

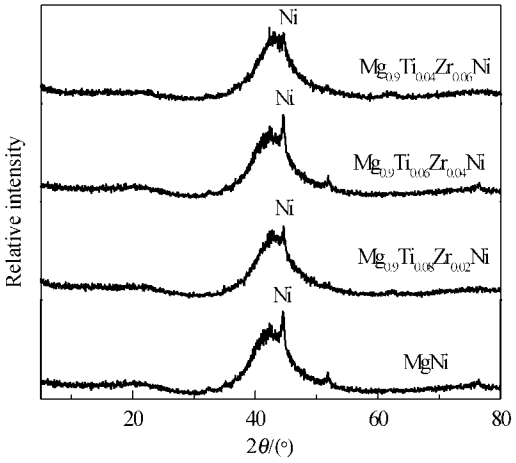

Figure 2 XRD pattern of MgNi, $Mg_{0.9}Ti_{0.1-x}Zr_xNi$ (x=0.02, 0.04, 0.06) by MA 80 h.

Figure 3 is XRD patterns of $Mg_{0.9}Ti_{0.06}Zr_{0.04}Ni$ surface modified or coated with graphite and $Mg_{0.9}Ti_{0.06}Zr_{0.04}Ni$ uncoated alloy. Compared to XRD patters of both alloys, the peak of the coated alloys is boarder and less intense, but the change is not very distinctive. The $Mg_{0.9}Ti_{0.06}Zr_{0.04}Ni$ alloy coating with graphite and uncoated $Mg_{0.9}Ti_{0.06}Zr_{0.04}Ni$ alloy were examined by SEM. As can be seen form the SEM image shown in Figures 4 and 5, after coated with graphite, some small graphite grains were absorbed on the surface of $Mg_{0.9}Ti_{0.06}Zr_{0.04}Ni$ alloy, and the other graphite grains penetrated into the inside surface alloy lattice. Figure 5

shows that there is a thin graphite sheet on the surface of $Mg_{0.9}Ti_{0.06}Zr_{0.04}Ni$ alloy.

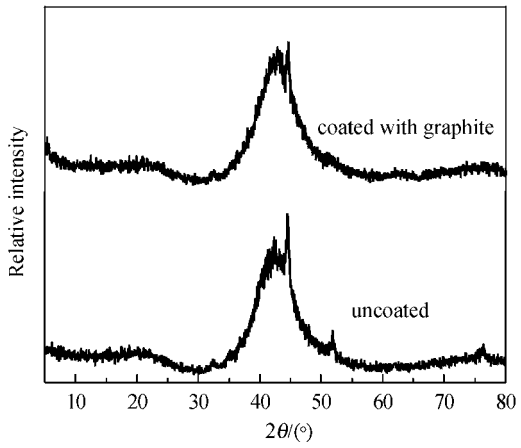

Figure 3 XRD patters of $Mg_{0.9}Ti_{0.06}Zr_{0.04}Ni$ coated with graphite and uncoated alloys.

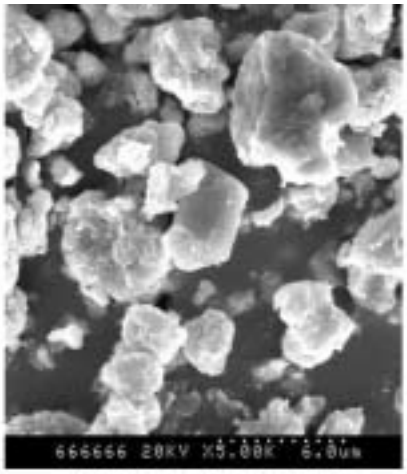

Figure 4 SEM micrograph of $Mg_{0.9}Ti_{0.06}Zr_{0.04}Ni$ alloy uncoated with graphite.

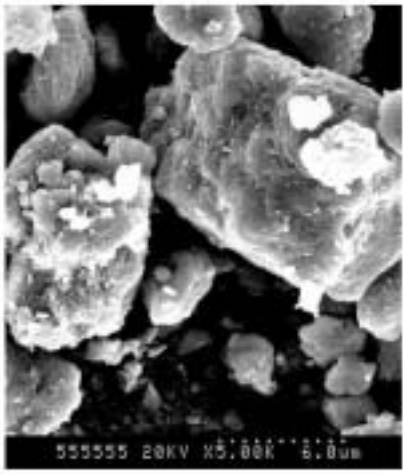

Figure 5 SEM micrograph of $Mg_{0.9}Ti_{0.06}Zr_{0.04}Ni$ alloy coated with graphite.

Charging/discharging characteristics

MA MgNi and $Mg_{0.9}Ti_{0.1-x}Zr_xNi$ (x=0.02, 0.04, 0.06) alloy possess good activation behavior, and all alloys reach their maximum discharge capacity at the first cycle. Figure 6 shows discharge capacities of those alloy electrodes. Compared to MgNi alloy, the discharge capacity of $Mg_{0.9}Ti_{0.08}Zr_{0.02}Ni$ and $Mg_{0.9}Ti_{0.06}Zr_{0.04}Ni$ alloys was increased. Especially, the $Mg_{0.9}Ti_{0.06}Zr_{0.04}Ni$ alloy has the maximum discharge capacity, which is 401.56 $mA{\cdot}h{\cdot}g^{-1}$ at a discharge density of 25 $mA{\cdot}h{\cdot}g^{-1}$ in the first cycle. The increasing discharge capacity indicates that partial substitution of alloying elements Ti and Zr for Mg has distinctively improved the discharge capacities of MgNi alloy. From Figure 6, a few substitution of Zr for Mg could improve the discharge capacities of x=0.02, 0.04 alloys, but much substitution of Zr for Mg decreased the discharge capacities of x=0.06 alloy. That is because, the atomic radius of Zr is larger than that of Mg, little partial Zr substitution atom penetrates into the alloy lattice so that it prefers a good channel for hydrogen diffusion. But there is not enough reason to excuse why much substitution of Zr for Mg decreased the discharge capacities of the x=0.06 alloy.

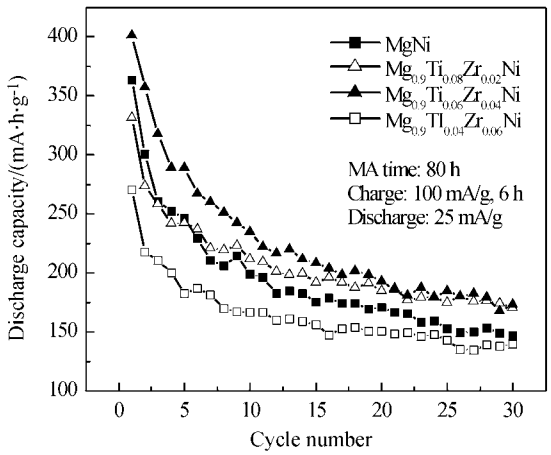

Figure 6 Discharge capacities of MgNi and $Mg_{0.9}Ti_{0.1-x}Zr_xNi$ (x =0.02, 0.04, 0.06) all electrodes.

Figure 7 shows cycle performance of MgNi and $Mg_{0.9}Ti_{0.1-x}Zr_xNi$ (x=0.02, 0.04, 0.06) alloy electrodes. The $Mg_{0.9}Ti_{0.1-x}Zr_xNi$ (x=0.02, 0.04, 0.06) alloy electrodes have better cycle life than MgNi alloy. With the substitution of Ti lower and the substitution of Zr higher, the cycle stability was decreased. It indicated that partial substitutions of Ti for Mg can improve the cycle performance of the alloys and the corruption of alloy in the alkali solution, but this partial substitutions of Ti can not improve the discharge capacity of the alloys. Iwakura *et al.*[8] reported that it is because in the process of discharge, Ti performed a thick sheet of oxidation that the partial substitution improved the anti-corruption ability of the alloys. This result agrees with the correlate study by Ye *et al.*[16] In conclusion at the MgNi type hydrogen storage alloys, little partial substitutions of Zr for Mg can improve the discharge capacities of the alloys, and

partial substitutions of Ti for Mg can improve the cycle performance of the alloy electrodes.

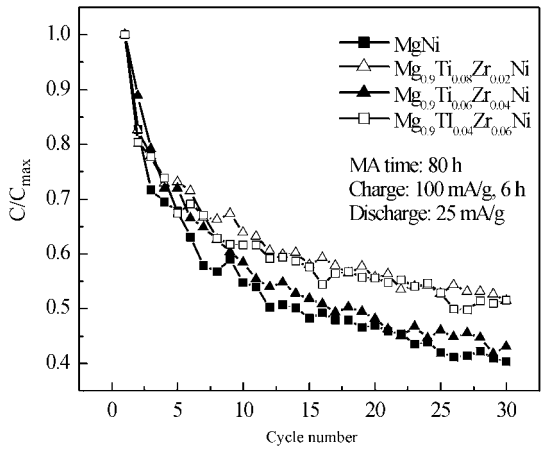

Figure 7 Cycle life of MgNi and $Mg_{0.9}Ti_{0.1-x}Zr_xNi$ (x=0.02, 0.04, 0.06) alloy electrodes.

Figure 8 is the XRD figure of $Mg_{0.9}Ti_{0.06}Zr_{0.04}Ni$ alloy electrode after 30 cycles charge-discharge. Except the Ni peak in this XRD pattern, we can see $Mg(OH)_2$ peak, which indicates that after 30 cycles, $Mg(OH)_2$ has been formed on the surface of the alloy electrode, decreasing the stability of $Mg_{0.9}Ti_{0.06}Zr_{0.04}Ni$ alloy electrode in alkali solution. This is because the corrosion outcomes surround the alloy particle to prevent them from contacting basal body and absorbing-desorbing hydrogen which consequently led to rapid decrease of alloy electrode capacity. Therefore, the form action of $Mg(OH)_2$ on the electrode surface is the main reason.

From Figure 9, we can see that both the discharge capacity and the cycle performance of the $Mg_{0.9}Ti_{0.06}Zr_{0.04}Ni$ alloy electrode were improved after MA 1 h with graphite. Graphite has a good surface modification effect on alloy to improve its electrochemical characteristics.

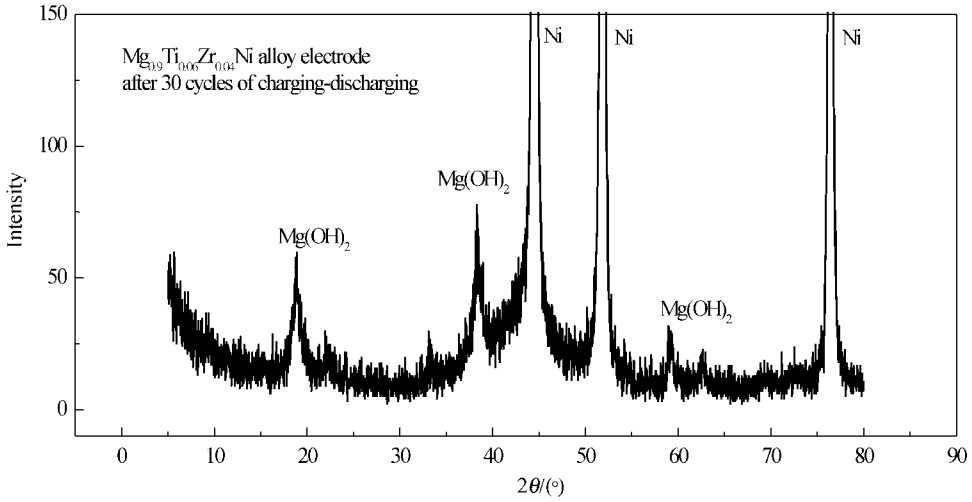

Figure 8 XRD figure of $Mg_{0.9}Ti_{0.06}Zr_{0.04}Ni$ alloy electrode after 30 cycles of charging-discharging.

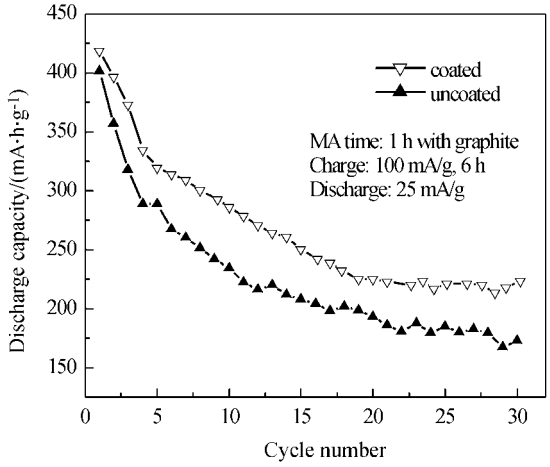

Figure 9 Discharge capacities of $Mg_{0.9}Ti_{0.06}Zr_{0.04}Ni$ alloy electrodes coated and uncoated with graphite.

The surface element distribution of the $Mg_{0.9}Ti_{0.06}Zr_{0.04}Ni$-graphite alloys (EDAX)

EDAX is a method to test the surface element distribution of the alloys. In order to further study the reasons for the improvement of anticorruption in the alkali solution, the coated with graphite and uncoated $Mg_{0.9}Ti_{0.06}Zr_{0.04}Ni$ alloys were tested by EDAX methods. Figure 10 is the EDAX pattern of uncoated $Mg_{0.9}Ti_{0.06}Zr_{0.04}Ni$ alloy, and Figure 11 is the EDAX pattern of that alloy coated with graphite.

As can be seen from Figures 10, 11 and Tables 1, 2, before and after coating with graphite, the mass and atom content of element Mg, Ni on the surface of the alloy decreased. Before and after alloys were coated with graphite, the mass proportion of Ni/Mg on the surface of the alloy increased from 2.052 to 2.056, and atom proportion of Ni/Mg increased from 0.8499 to 0.8515. With the content of Ni/Mg increasing, the mass and atom content of Mg on the alloy surface decreased,

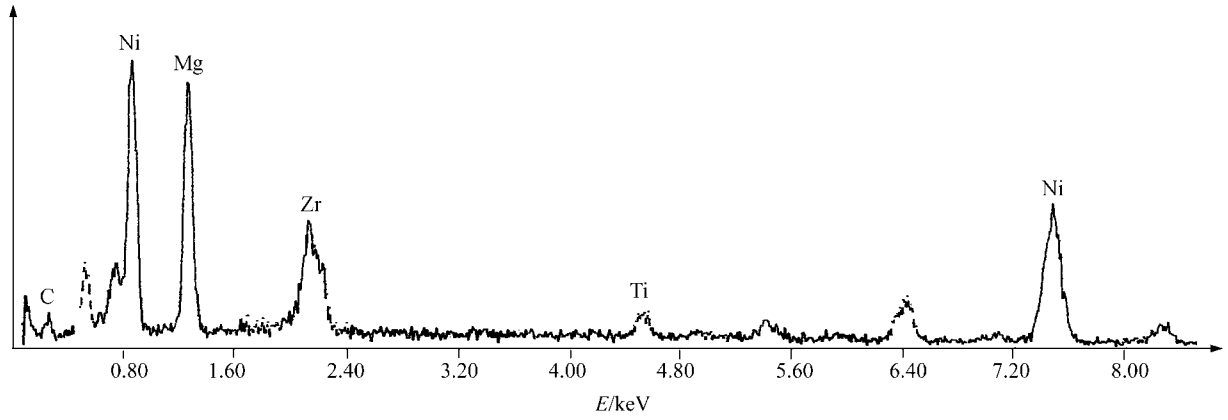

Figure 10 the EDAX pattern of uncoated $Mg_{0.9}Ti_{0.06}Zr_{0.04}Ni$ alloy.

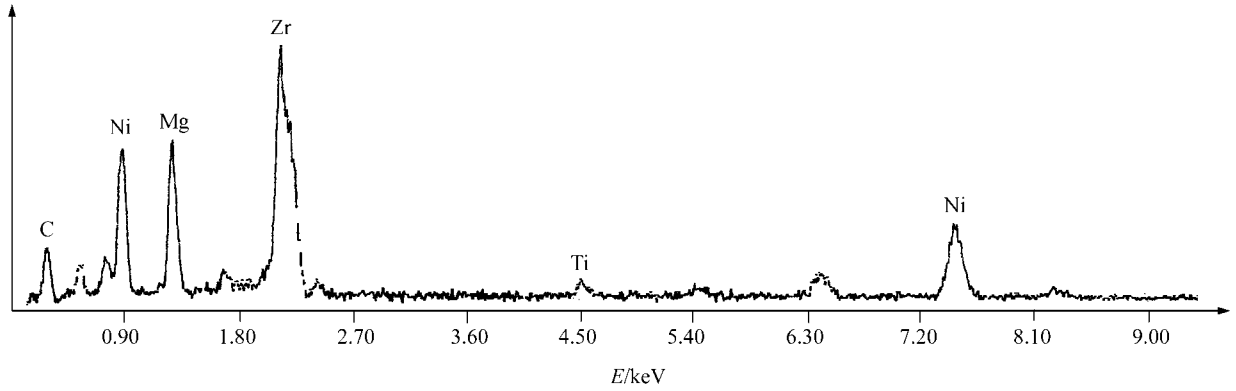

Figure 11 the EDAX pattern of coated $Mg_{0.9}Ti_{0.06}Zr_{0.04}Ni$ alloy.

Table 1 The mass content of partial surface elements of the $Mg_{0.9}Ti_{0.06}Zr_{0.04}Ni$ coated with graphite (wt%)

	C	Mg	Ni
Before coated	11.86	25.56	52.46
After coated	33.63	16.37	33.66

Table 2 The atom content of partial surface elements of the $Mg_{0.9}Ti_{0.06}Zr_{0.04}Ni$ coated with graphite (wt%)

	C	Mg	Ni
Before coated	32.10	34.17	29.04
After coated	65.82	15.83	13.48

which decreased the corrupted probability of Mg in alkali solution. Therefore, we can draw the conclusion that the mass and atom proportion of Ni/Mg on the surface of the $Mg_{0.9}Ti_{0.06}Zr_{0.04}Ni$ alloy is the main reason for the improving of anticorruption characteristic. In addition, graphite coated sheet on the alloy surface protected the alloy from corruption in the alkali solution at the same time improving the anticorruption of $Mg_{0.9}Ti_{0.06}Zr_{0.04}Ni$ alloy.

Conclusions

(1) The Mg-based hydrogen storage alloys MgNi and $Mg_{0.9}Ti_{0.1-x}Zr_xNi$ (x=0.02, 0.04, 0.06) were successful prepared by means of mechanical alloying (MA). The XRD patters indicated that all the alloy were almost amorphized and the partial substitution of Zr for Mg in MgNi type alloys can promote the extent of amorphism in those alloys.

(2) In all alloys prepared in this work, $Mg_{0.9}Ti_{0.06}Zr_{0.04}Ni$ alloy electrode has a maximum discharge capacity, but the cycle life of this alloy is not very satisfactory. Discharge capacities of $Mg_{0.9}Ti_{0.1-x}Zr_xNi$ (x= 0.02, 0.04, 0.06) alloys were improved by little Zr adding and cycle life of the alloy was stabilized by Ti adding.

(3) Both of the discharge capacity and cycle performace of $Mg_{0.9}Ti_{0.06}Zr_{0.04}Ni$ alloy were improved by surface modification or coating with 10 wt% graphite. The pattern of XRD indicated that the main amorphous structure is not changed much by coating with graphite, but the SEM pattern of the $Mg_{0.9}Ti_{0.06}Zr_{0.04}Ni$ coated alloy showed that little grains of graphite were penetrated into the inside crystal structure of the alloy surface. And the SEM pattern also showed that there was a thin sheet on the alloy surface, and the sheet protected and shielded Mg from corruption in the alkali solution, thus it could improve the anti-corrosion behavior of the $Mg_{0.9}Ti_{0.06}Zr_{0.04}Ni$ alloy electrode.

(4) The EDAX pattern indicated that the mass and

atom proportion of Ni/Mg were increased, which decreased the corrupted probability of the Mg in alkali solution and that further illuminated that the cycle performance of the $Mg_{0.9}Ti_{0.06}Zr_{0.04}Ni$ alloy electrode is improved by coating with graphite.

References

1 Yuan, H.; Li, Q.; Song, H.; Wang, Y.; Liu, J. *J. Alloys Comp.* **2003**, *353*, 322.

2 Zhang, Y.; Lei, Y.; Chen, L.; Yuan, J.; Zhang, Z.; Wang, Q. *J. Alloys Comp.* **2002**, *337*, 296.

3 Goo, N. H.; Jeong, W. T.; Lee, K. S. *J. Power Souces* **2000**, *87*, 118.

4 Wang, L.; Yuan, H.; Wang, Y.; Li, Q.; Song, H.; Yang, H. J. *J. Alloys Comp.* **2002**, *336*, 297.

5 Song, M. Y. *Inter. J. Hydrogen Energy* **2003**, *28*, 403.

6 Han, S.; Lee, P. S.; Lee, J.; Zuttel, A.; Schlapbach, L. *J. Alloys Comp.* **2000**, *306*, 219.

7 Liang, G.; Huot, J.; Boily, S.; Neste, A. V.; Schulz, R. *J. Alloys Comp.* **1999**, *292*, 247.

8 Iwakura, C.; Inoue, H. ; Zhang, S. G.; Nohara, S. *J. Alloys Comp.* **1998**, *270*, 142.

9 Liu, W.; Wu, H.; Lei, Y.; Wang, Q.; Wu, J. *J. Alloys Comp.* **1997**, *252*, 234.

10 Iwakura, C.; Nohara, S.; Inoune, H.; Fukumoto, Y. *Chem. Commun.* **1996,** *1*, 1831.

11 Han, S.; Jiang, J.; Park, J.; Tang, K.; Chin, E. J.; Lee, J. *J. Alloys Comp.* **1999**, *285*, L8-L11.

12 Iwakura, C. ; Nohara, S.; Inoue, H. *Solid State Ionics* **2002,** *148*, 499.

13 Yuan, H.; Wang, L.; Cao, R.; Wamg, Y.; Zhang, Y.; Yan, D.; Zhang, W.; Gong, W. *J. Alloys Comp.* **2000**, *309*, 208.

14 Goo, N. H.; Lee, K. S. *Inter. J. Hydrogen Energy* **2002**, *27*, 433.

15 Chakk, Y.; Berger, S.; Weis, B.-Z.; Brook-Levinson, E. *Acta Mater.* **1994**, *42*, 3679.

16 Ye, H.; Lei, Y. Q.; Chen, L. S.; Zhang, H. *J. Alloys Comp.* **2000**, *311*, 194.

(E0308227 ZHAO, X. J.)